Title	In vivo manganese-enhanced MRI and diffusion tensor imaging of developing and impaired visual brains
Author(s)	Chan, KC; Cheng, JS; Fan, S; Zhou, IY; Wu, EX
Citation	The 33rd Annual International Conference of the IEEE Engineering in Medicine and Biology Society (EMBC 2011), Boston, MA., 30 August-3 September 2011. In IEEE Engineering in Medicine and Biology Society Conference Proceedings, 2011, p. 7005-7008
Issued Date	2011
URL	http://hdl.handle.net/10722/158763
Rights	IEEE Engineering in Medicine and Biology Society Conference Proceedings. Copyright © IEEE.

33rd Annual International Conference of the IEEE EMBS
Boston, Massachusetts USA, August 30 - September 3, 2011

In vivo Manganese-enhanced MRI and Diffusion Tensor Imaging of Developing and Impaired Visual Brains

Kevin C. Chan, Joe S. Cheng, Shujuan Fan, Iris Y. Zhou, and Ed X. Wu*

Abstract— **This study explored the feasibility of high-resolution Mn-enhanced MRI (MEMRI) and diffusion tensor imaging (DTI) for in vivo assessments of the development and reorganization of retinal and visual callosal pathways in normal neonatal rodent brains and after early postnatal visual impairments. Using MEMRI, intravitreal Mn^{2+} injection into one eye resulted in maximal T1-weighted hyperintensity in neonatal contralateral superior colliculus (SC) 8 hours after administration, whereas in adult contralateral SC signal increase continued at 1 day post-injection. Notably, mild but significant Mn^{2+} enhancement was observed in the ipsilateral SC in normal neonatal rats, and in adult rats after neonatal monocular enucleation (ME) but not in normal adult rats. Upon intracortical Mn^{2+} injection to the visual cortex, neonatal binocularly-enucleated (BE) rats showed an enhancement of a larger projection area, via the splenium of corpus callosum to the V1/V2 transition zone of the contralateral hemisphere in comparison to normal rats. For DTI, the retinal pathways projected from the enucleated eyes possessed lower fractional anisotropy (FA) 6 weeks after BE and ME. Interestingly, in the optic nerve projected from the remaining eye in ME rats a significantly higher FA was observed compared to normal rats. The results of this study are potentially important for understanding the axonal transport, microstructural reorganization and functional activities in the living visual brain during early postnatal development and plasticity in a global and longitudinal setting.**

I. INTRODUCTION

The rodents are an excellent model for understanding the developmental and pathophysiological mechanisms in the visual system [1-3]. Along the visual pathways, the retinocollicular projection between retina and the superficial layers of superior colliculus (SC), and the retinogeniculate projection between retina and lateral geniculate nucleus (LGN) are commonly used for evaluating the mechanisms of retinotopic map formation, neurodegeneration and plasticity in the subcortical brain [4-6]. In addition, the visual cortex is known to communicate interhemispherically via the splenium of corpus callosum, which is sensitive to plastic changes during early postnatal development [7]. Despite the increasing number of studies investigating retinotopic and callosal projections in visual brain development and disorders [4], limited studies have been available for in vivo, high-resolution and systematic investigations of the developmental and plastic changes in the cortical and subcortical visual nuclei. Mn^{2+} has been increasingly used as a T_1-weighted contrast agent for in vivo neuronal tract tracing [3, 8] and functional brain mapping at lamina levels in the adult brains [5, 9]. In this study, we explore the capability of high-resolution Mn-enhanced MRI (MEMRI) for in vivo, global and longitudinal assessments of the retinal and visual callosal projections in normal neonatal brains and after early postnatal visual impairments. In addition, diffusion tensor imaging (DTI) was acquired to examine the effect of early visual impairment on the microstructural integrity in cerebral white matter in both anterior and posterior visual brains, and to complement the MEMRI findings. Results of this study are potentially important for understanding the axonal transport, microstructural reorganization and functional activities in the living visual brain during early postnatal development and plasticity.

Manuscript received June 19, 2011. This work was supported in part by the Hong Kong Research Grant Council and The University of Hong Kong CRCG grant.

Kevin C. Chan, Joe S. Cheng, Shujuan Fan, Iris Y. Zhou and Ed X. Wu are with the Laboratory of Biomedical Imaging and Signal Processing and the Department of Electrical and Electronic Engineering, The University of Hong Kong, Hong Kong SAR, China (e-mail: chuenwing.chan@fulbrightmail.org, chengshi06@gmail.com, sjfan@eee.hku.hk, iriszhou@eee.hku.hk, ewu@eee.hku.hk). Kevin C. Chan is also with the Department of Ophthalmology, UPMC Eye Center, Eye and Ear Institute, Ophthalmology and Visual Science Research Center, University of Pittsburgh School of Medicine, Pittsburgh, PA, USA.

*Ed X. Wu is the corresponding author to provide phone: (852) 2819-9713; fax: (852) 2819-9711.

II. MATERIALS AND METHODS

A. Animal Preparation

Sprague-Dawley rats (N=56) were divided into 7 groups. In the normal brain development groups, 6 rats at postnatal days (P) 1, 5, 10 and 60 each were injected intravitreally with 100mM $MnCl_2$ solution into one eye, and MEMRI was performed 8 hours (Hr8) and 1 day (D1) after Mn^{2+} administration. Considering the increasing vitreal volume and decreasing retinal ganglion cell and optic nerve counts in rats with age [10, 11], the Mn^{2+} injection volume was chosen to be 0.5, 1.0, 1.5 and 2.0 μL respectively at P1, P5, P10 and P60. This resulted in vitreal concentrations below toxic levels shown to inhibit terminal field enhancement in both rat and

mouse superior colliculi (SC) in adults [12, 13]. Given the similar vitreal volumes and brain sizes between adult mice and neonatal rats at P1 [10], MEMRI was also performed to 6 P60 C57BL/6J mice after intravitreal Mn^{2+} injection into one eye at the same dosage as P1 rats. Four age-matched rats/mice without Mn^{2+} injection were scanned from each age group as a control (CTRL).

In the visually impaired groups, neonatal binocular enucleation (BE, n=6) and monocular enucleation to the right eye (ME, n=6) were performed at P1. DTI was acquired to the BE, ME and 6 CTRL rats at 6 weeks old. At P60, MEMRI was performed 1 day after intravitreal Mn^{2+} injection to the remaining left eye of the ME group at the same dosage as for normal P60 rats. At about P90, Mn^{2+} was injected intracortically to 4 BE and another 4 CTRL rats, at the V1/V2 border of one hemisphere at a dose of 100nL at 100mM. MEMRI was performed 1 hour (Hr1) and 1 day (D1) after Mn^{2+} administration.

B. MRI Protocols

All MRI measurements were acquired utilizing a 7 Tesla Bruker scanner. Under inhaled isoflurane anaesthesia (3% induction and 1% maintenance), animals were kept warm under circulating water at 37°C with continuous monitoring of the respiration rate. For retinal projection studies, 2D T1-weighted (T1W) fast spin-echo pulse sequence was acquired at an oblique orientation parallel to the superficial layers of SC, with repetition time/echo time (TR/TE) = 400/7.5 ms, field of view/slice thickness (FOV/th) = 20x20 mm^2/0.5 mm for neonatal rats and adult mice and 32x32 mm^2/0.8 mm for adult rats, matrix resolution (MTX) = 200x200, number of slices = 9, echo train length (ETL) = 4 and number of excitations (NEX) = 60. Total scan time was 15 mins. For callosal projection studies, similar 2D T1W imaging protocol was applied in a coronal view covering the visual cortex, but with TR/TE= 455/8.5 ms, MTX = 256x256 and NEX = 42. T2WI was performed under the same spatial dimensions, with TR/TE = 4200/38.7 ms, ETL = 8 and NEX = 2; For DTI, 4-shot spin-echo echo-planar-imaging diffusion weighted images were acquired with FOV/th = 32x32 mm^2/1 mm, MTX = 128x128, number of slices = 15, TR/TE = 3750/30 ms, b = 0 and 1000 s/mm^2 and 30 diffusion directions.

C. Data Analysis

For normal brain development study, T1W signal intensities (SI) in the superficial layers of SC were measured from both hemispheres in each group using ImageJ v1.43u, and were normalized to a non-visual area in the brain. Mn^{2+} enhancement was quantified by calculating the rate of signal increase at Hr8 and D1 compared to CTRL animals. Values of each brain nuclei in the same age groups were compared using two-tailed unpaired or paired t-tests. For brain plasticity study, T1W SI of both SC in ME rats were compared to those of age-matched CTRL rats using unpaired t-tests. The visual callosal projection in the hemisphere contralateral to intracortical Mn^{2+} injection was evaluated qualitatively between BE and CTRL groups in T1W images. For DTI, fractional anisotropy (FA) maps were obtained using DTIStudio v2.30 after co-registration. FA values along the major visual pathways projected from the left eye [left prechiasmatic optic nerve (L-PON), and right anterior (R-AOT) and posterior optic tract (R-POT)] and from the right eye [right prechiasmatic optic nerve (R-PON), and left anterior (L-AOT) and posterior optic tract (L-POT)] were measured using ImageJ, and were compared among BE, ME and CTRL groups using unpaired t-tests. Results were considered significant when $p<0.05$.

III. Results

A. MEMRI of Early Postnatal Visual Development in Retinal Projections

In the T1W images in Fig. 1, intravitreal Mn^{2+} injection into one eye resulted in T1W hyperintensity consistently in the ipsilateral retina and optic nerve, and contralateral SC and LGN in all neonatal (P1, P5 and P10) and adult (P60) brains at Hr8. Interestingly, while the T1WSI of contralateral SC continued to increase in the adult rats ($p<0.05$) at D1, or remained the same in the adult mice ($p>0.05$), the SI of contralateral SC dropped significantly in the neonatal rats at D1 compared to Hr8. In the ipsilateral SC, a small but significant increase in SI could also be observed in the neonatal brains at Hr8, as well as the adult mice at D1.

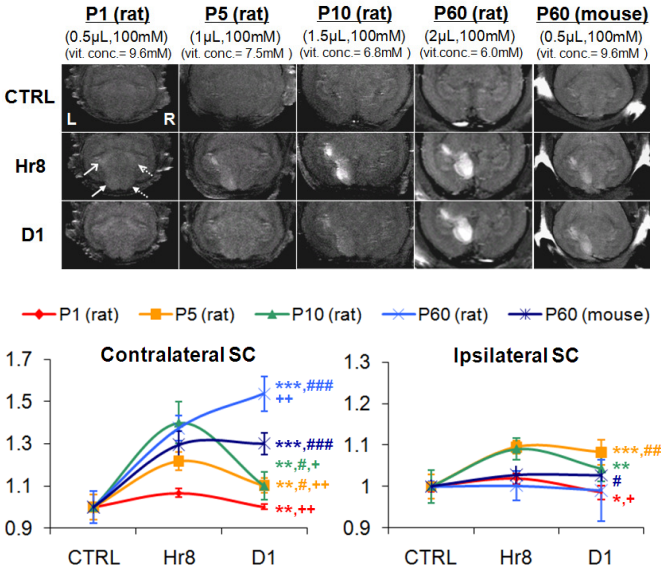

Fig. 1: (Top) Maximal intensity projection of 2D T1W images of normally developing posterior visual brain nuclei at postnatal days (P) 1, 5, 10 and 60 in rats, and at P60 in mice with (Hr8 and D1) and without (CTRL) Mn^{2+} injection to the right eyes. Slices were oriented to cover the contralateral left superior colliculus (SC) (solid arrow), left lateral geniculate nucleus (LGN) (solid, open arrow), and ipsilateral right SC (dashed arrow) and right LGN (dashed open arrow) (vit. conc.: vitreal concentration). (Bottom) Quantitative analyses of T1W signal increase in contralateral and ipsilateral SC in the same age groups. (Two-tailed unpaired t-test between CTRL and Hr8, *p<0.05; **p<0.01; ***p<0.001; Two-tailed unpaired t-test between CTRL and D1, $^{\#}$p<0.05; $^{\#\#}$p<0.01; $^{\#\#\#}$p<0.001; Two-tailed paired t-test between Hr8 and D1, $^{+}$p<0.05; $^{++}$p<0.01; $^{+++}$p<0.001)

B. MEMRI and DTI of Neural Plasticity in Retinal Projections

In the anatomical T2W images, shrinkage of SC and LGN was observed in both hemispheres of BE rats and in the left hemisphere of ME rats (data not shown). In MEMRI in Fig. 2, intravitreal Mn^{2+} injection into the left eye resulted in T1W enhancement in the entire superficial layers of the contralateral right SC in both ME and CTRL rats at P60. Mild enhancement could also be observed in the SC ipsilateral to the remaining left eye in the ME group (arrows), but was not apparent in CTRL group. Quantitative analysis confirmed a significantly higher T1W SI in the superficial layers of ipsilateral left SC in ME animals than CTRL animals ($p<0.05$). No significant SI difference was observed in contralateral right SC between ME and CTRL ($p>0.05$). For DTI, the PON, AOT and POT could be visualized in both hemispheres of the BE, ME and CTRL groups each in the FA maps in Fig. 3 (Top). Quantitative analyses in Fig. 3 (Bottom) indicated a significantly lower FA along the retinal pathways projected from the enucleated eyes in BE and ME rats compared to CTRL rats. Interestingly, a significantly higher FA was found in the L-PON projected from the remaining left eye of the ME rats, in comparison to both BE and CTRL rats.

C. MEMRI of Neural Plasticity in Visual Callosal Projections

Upon intracortical Mn^{2+} injection to the visual cortex of normal adult brains (Fig. 4), T1W hyperintensity was observed at the SC and dorsal LGN of the ipsilateral hemisphere, the splenium of corpus callosum, and the V1/V2 transition zone of the contralateral hemisphere at D1. Notably, intracortical Mn^{2+} injection to the BE adult brains appeared to enhance a larger area of callosal projection at the V1/V2 border, which extended medially toward the primary visual cortex in the contralateral hemisphere (Fig. 4).

IV. Discussions

The results of the MEMRI study in normal neonatal visual brains demonstrated the feasibility of in vivo, high-resolution MEMRI for assessing the retinal projection in SC and LGN in the early postnatal brains before natural eyelid opening. They also suggested the differential transport mechanisms of Mn^{2+}

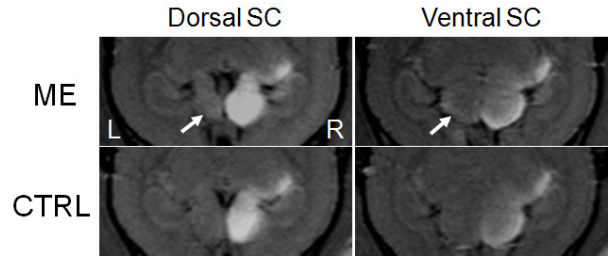

Fig. 2: T1W images of the SC at 1 day after Mn^{2+} intravitreal injection into the left eyes of monocularly enucleated (ME) and control animals at P60. Robust Mn enhancement could be observed in the entire right dorsal SC, and at the border of the right ventral SC in all groups. Note also the mild enhancement in the superficial layers of left SC in the ME group (arrows).

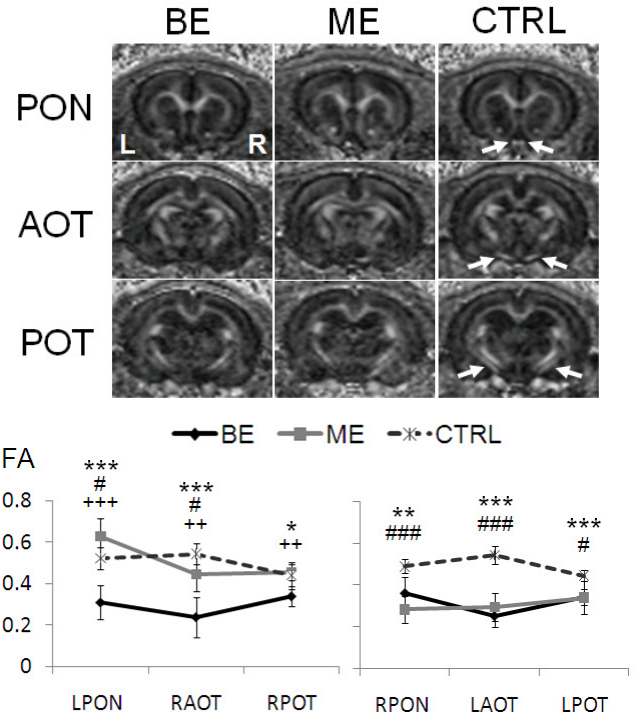

Fig. 3: (Top) Fractional anisotropy (FA) maps of the experimental groups (BE, ME) and the control group (CTRL) at the levels of prechiasmatic optic nerve (PON), anterior optic tract (AOT), and posterior optic tract (POT) (arrows in CTRL) at 6 weeks old. (Bottom) Comparisons of FA values along the visual retinal pathways projected from the left (left) and right eyes (right). (Two-tailed unpaired t-test between BE and CTRL, *p<0.05, **p<0.01, ***p<0.001; Two-tailed unpaired t-test between ME and CTRL, $^{\#}$p<0.05, $^{\#\#}$p<0.01, $^{\#\#\#}$p<0.001; Two-tailed unpaired t-test between BE and ME, $^{+}$p<0.05)

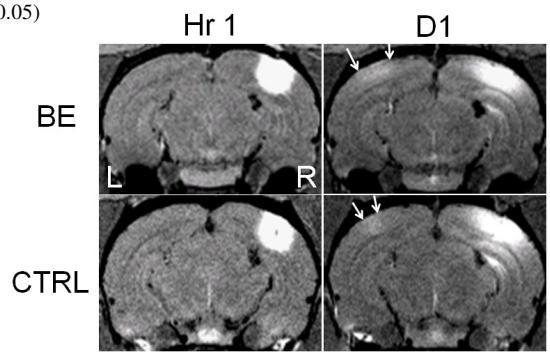

Fig. 4: Coronal T1W images of the visual cortex at 1 hour (Hr1) and 1 day (D1) after intracortical Mn^{2+} injection to V1/V2 border in the right hemisphere of BE and CTRL rats at around P90. Note the larger area of projection near the V1/V2 border in the contralateral left hemisphere of BE rats compared to CTRL rats (arrows).

at the nerve terminals between neonatal and adult visual pathways. The T1W hyperintensity in the ipsilateral retina and optic nerve of neonatal brains indicated the presence of Mn^{2+} uptake and transport along the neonatal retinal pathway in spite of the absence of direct light input to the eye. Despite a lower rate of fast axonal transport [14], our observation of the earlier occurrence of maximal Mn^{2+} enhancement in contralateral neonatal SC at Hr8 than adult SC at D1 or later, might be ascribed partially to the lower activity in the functionally immature retina and optic nerve synapses at SC [14], the higher diffusion out of the unmyelinated fibers of the developing optic tracts and superficial SC [15], and the higher blood-ocular or blood-brain barrier permeability in the immature rat brains [16]. The ipsilateral retinocollicular projections of the newborn rats and pigmented adult mice are known to be more prominent than those in the normal adult albino rats [7, 17, 18]. In this study, the higher T1W SI observed in the SC ipsilateral to Mn^{2+}-injected eyes of neonatal normal rats and adult normal mice, but not adult normal rats likely indicated the high sensitivity of MEMRI for detecting such uncrossed retinal projections in the developing brains across different rodent species.

It has been suggested that younger brains are more capable of rewiring the neural connections than older brains. Previous histological studies on early visual impairments showed that neonatal unilateral eye removal (ME) resulted in a significant increase in the number of aberrant, ipsilaterally projecting retinal ganglion cells in the remaining eye compared to normal rats [7, 19, 20]. The interhemispheric connections in visual cortex might also be reorganized upon neonatal BE [7]. The current MEMRI studies on ME and BE demonstrated the capability of MEMRI in detecting neural plasticity of the uncrossed retinal projections in SC in vivo after ME, and the expanded visual callosal projections at the V1/V2 border after BE. Whether the higher FA in the left optic nerve (L-PON) of ME rats in DTI was related to the retention of optic nerve axons from the ipsilaterally projecting retinal ganglion cells of the left eye [7] remained to be elucidated. The lower FA in PON, AOT and POT of BE and ME rats suggested neurodegeneration or immaturity of the afferent fibers projected from the enucleated eyes [7]. On the other hand, the similar Mn^{2+} enhancements in contralateral right SC between ME and CTRL groups were likely ascribed to the comparable microstructural integrity of crossed optic tract fibers (R-AOT and R-POT) from the left, untreated eyes in ME and CTRL rats.

V. Conclusions

The current results demonstrated the feasibility of MEMRI and DTI for assessing the retinal organiziations in early postnatal brains in vivo before natural eyelid opening, and for detecting the neural plasticity of the uncrossed retinal projection and the visual callosal projection upon early postnatal visual impairments. Future MEMRI and DTI studies are envisioned that measure the development and reorganization of retinal and visual callosal projections in disease, plasticity, drug interventions and genetic modifications in a global and longitudinal setting.

References

[1] K. C. Chan, *et al.*, "In vivo multiparametric magnetic resonance imaging and spectroscopy of rodent visual system," *J Integr Neurosci,* vol. 9, pp. 477-508, Dec 2010.

[2] K. C. Chan, *et al.*, "GD-DTPA enhanced MRI of ocular transport in a rat model of chronic glaucoma," *Exp Eye Res,* vol. 87, pp. 334-341, Jun 28 2008.

[3] K. C. Chan, *et al.*, "Evaluation of the retina and optic nerve in a rat model of chronic glaucoma using in vivo manganese-enhanced magnetic resonance imaging," *Neuroimage,* vol. 40, pp. 1166-74, Apr 15 2008.

[4] D. D. O'Leary and T. McLaughlin, "Mechanisms of retinotopic map development: Ephs, ephrins, and spontaneous correlated retinal activity," *Prog Brain Res,* vol. 147, pp. 43-65, 2005.

[5] K. C. Chan, *et al.*, "In vivo retinotopic mapping of superior colliculus using manganese-enhanced magnetic resonance imaging," *Neuroimage,* vol. 54, pp. 389-395 2011/01/01 2011.

[6] K. C. Chan, *et al.*, "Functional MRI of postnatal visual development in normal and hypoxic-ischemic-injured superior colliculi," *Neuroimage,* vol. 49, pp. 2013-20, Feb 1 2010.

[7] B. Dreher, *et al.*, "The morphology, number, distribution and central projections of Class I retinal ganglion cells in albino and hooded rats," *Brain Behav Evol,* vol. 26, pp. 10-48, 1985.

[8] R. G. Pautler, *et al.*, "In vivo neuronal tract tracing using manganese-enhanced magnetic resonance imaging," *Magn Reson Med,* vol. 40, pp. 740-8, Nov 1998.

[9] X. Yu, *et al.*, "In vivo auditory brain mapping in mice with Mn-enhanced MRI," *Nat Neurosci,* vol. 8, pp. 961-8, Jul 2005.

[10] O. Sha and W. H. Kwong, "Postnatal Developmental Changes of Vitreous and Lens Volumes in Sprague-Dawley Rats," *Neuroembryol Aging,* vol. 4, pp. 183-188, 2006.

[11] K. Lam, *et al.*, "Loss of axons from the optic nerve of the rat during early postnatal development," *Brain Res,* vol. 255, pp. 487-91, Mar 1982.

[12] A. S. Lowe, *et al.*, "Quantitative manganese tract tracing: dose-dependent and activity-independent terminal labelling in the mouse visual system," *NMR Biomed,* vol. 21, pp. 859-67, Oct 2008.

[13] M. Thuen, *et al.*, "Manganese-enhanced MRI of the rat visual pathway: acute neural toxicity, contrast enhancement, axon resolution, axonal transport, and clearance of Mn(2+)," *J Magn Reson Imaging,* vol. 28, pp. 855-65, Oct 2008.

[14] S. C. Specht, "Axonal transport in the optic system of neonatal and adult hamsters," *Exp Neurol,* vol. 56, pp. 252-64, Aug 1977.

[15] S. S. Warton and D. G. Jones, "Postnatal development of the superficial layers in the rat superior colliculus: a study with Golgi-Cox and Kluver-Barrera techniques," *Exp Brain Res,* vol. 58, pp. 490-502, 1985.

[16] C. L. Farrell and W. Risau, "Normal and abnormal development of the blood-brain barrier," *Microsc Res Tech,* vol. 27, pp. 495-506, Apr 15 1994.

[17] L. K. Laemle and A. R. Labriola, "Retinocollicular projections in the neonatal rat: an anatomical basis for plasticity," *Brain Res,* vol. 255, pp. 317-22, Feb 1982.

[18] U. C. Drager and J. F. Olsen, "Origins of crossed and uncrossed retinal projections in pigmented and albino mice," *J Comp Neurol,* vol. 191, pp. 383-412, Jun 1980.

[19] S. O. Chan and L. S. Jen, "Enlargement of uncrossed retinal projections in the albino rat: additive effects of neonatal eye removal and thalamectomy," *Brain Res,* vol. 461, pp. 163-8, Sep 27 1988.

[20] I. Hayakawa and H. Kawasaki, "Rearrangement of retinogeniculate projection patterns after eye-specific segregation in mice," *PLoS One,* vol. 5, p. e11001.